Electron-Phonon Coupling and a Polaron in the *t*-*J* Model: From the Weak to the Strong Coupling Regime

A. S. Mishchenko[1,2] and N. Nagaosa[1,3]

[1]*CREST, Japan Science and Technology Agency (JST), AIST, 1-1-1, Higashi, Tsukuba 305-8562, Japan*
[2]*RRC "Kurchatov Institute," 123182, Moscow, Russia*
[3]*CREST, Department of Applied Physics, The University of Tokyo, 7-3-1 Hongo, Bunkyo-ku, Tokyo 113, Japan*

(Received 17 November 2003; published 12 July 2004)

We present numeric results for ground state and angle resolved photoemission spectra (ARPES) for a single hole in the *t*-*J* model coupled to optical phonons. The systematic-error-free diagrammatic Monte Carlo method is employed where the Feynman graphs for the Matsubara Green function in imaginary time are summed up completely with respect to phonon variables, while magnetic variables are subjected to the noncrossing approximation. We obtain that at electron-phonon coupling constants relevant for high T_c cuprates the polaron undergoes a self-trapping crossover to the strong-coupling limit and theoretical ARPES demonstrate features observed in experiment: A broad peak in the bottom of the spectra has momentum dependence which coincides with that of a hole in the pure *t*-*J* model.

DOI: 10.1103/PhysRevLett.93.036402 PACS numbers: 71.10.Fd, 02.70.Ss, 71.38.–k, 79.60.–i

In the context of the broad interest in challenging the properties of the high-T_c superconductors, a single hole in the Mott insulator has been studied extensively in terms of the *t*-*J* model:

$$\hat{H}_{t\text{-}J} = -t\sum_{\langle ij\rangle s} c_{is}^{\dagger}c_{js} + J\sum_{\langle ij\rangle}(\mathbf{S}_i\mathbf{S}_j - n_i n_j/4), \qquad (1)$$

where $c_{j\sigma}$ is the projected (to avoid double occupancy) fermion annihilation operator, $n_i < 2$ is the occupation number, $\mathbf{S}_i$ is the spin-1/2 operator, and $\langle ij\rangle$ denotes nearest-neighbor sites in the two-dimensional lattice. Different theoretical approaches (for review and recent studies, see Refs. [1–4]) give consistent results for the Lehman spectral function (LSF) $L_{\mathbf{k}}(\omega) = -\pi^{-1}\Im G_{\mathbf{k}}(\omega)$ of the Green function $G_{\mathbf{k}}(\omega)$. Namely, the LSFs at all momenta have a quasiparticle (QP) peak in the low energy part together with a broad incoherent continuum extending up to the energy scale of the order of t. The sharp QP peak in the LSF of the ground state at momentum $\mathbf{k} = (\pi/2, \pi/2)$ has the weight $Z \sim J/t$. This QP peak is sharp at all momenta and its energy dispersion has the bandwidth $W_{J/t} \sim J$. The more advanced t-t'-t''-J model takes into account long range hopping amplitudes t' and t'' which alter the bandwidth and dispersion of the QP resonance [5–11]. It was shown [5] that, depending on the parameters of the t-t'-t''-J model, the QP peak can be either enhanced or completely suppressed at a large part of the Brillouin zone. However, at parameters which are needed for description of angle resolved photoemission spectra (ARPES) measurements on carefully studied [12] $Sr_2CuO_2Cl_2$ ($J/t \approx 0.4$, $t'/t \approx -0.3$, see [6–8]), the QP peak remains well defined for all momenta [5,13,14]. Possible damping of the peak [5], in contrast to experiment, is much less than the QP bandwidth. Therefore, the properties of the QP peak in the t-t'-t''-J model at realistic parameters are the same as in the generic *t*-*J* model.

Experimentally, ARPES in the undoped cuprates revealed the LSF of a single hole [10,11] and observed that dispersion of the lowest peak in the LSF is in good agreement with the theoretical predictions of the t-t'-t''-J model [6–11]. The puzzling point is that, in contrast to the theory, experiments never show sharp QP resonance, and a broad peak with the width of the order of 0.1–0.5 eV ($\approx t$) is observed instead. Note that broadening is seen just in undoped systems where the ground state of the single hole is the lowest energy state in the Hilbert space of the $(N-1)$-electron problem. One can rule out the possibility of an extrinsic origin of this width since the doping introduces further disorder, while a sharper peak is observed in the overdoped region.

The role of electron-phonon (*e*-ph) coupling has gained recent renewed interest. One reason is that the ARPES data in doped metallic cuprates revealed the energy dispersion strongly renormalized by *e*-ph interaction [11]. Besides, the strong *e*-ph interaction is crucial for explanation of renormalization and line shapes of phonons observed in neutron scattering experiments [15]. In addition, the large isotope effect on T_c for underdoped cuprates and on the superfluid density at the optimal doping suggests the vital role of *e*-ph coupling [16].

Strong and intermediate coupling regimes of *e*-ph interaction in the *t*-*J* model cannot be studied, neither by exact diagonalization [17] on small clusters nor by self-consistent Born approximation (SCBA), where both magnon and phonon propagators are subjected to noncrossing approximation (NCA) which neglects the vertex corrections [13,18,19]. The small system size implies a discrete spectrum and, hence, neither crossover from large to small size polaron nor the problem of linewidth in ARPES can be addressed in the former approach. The latter method omits the Feynman diagrams with mutual crossing of phonon propagators and, hence, neglects the vertex corrections which are crucial for treating the e-ph interaction in the strong-coupling regime (SCR). One can use the NCA for the interaction of the hole with magnetic system because spin $S = 1/2$ cannot flip more than one time, and the magnon cloud around the hole saturates. To the contrary, phonon-phonon noncrossing approximation (PPNCA) fails for SCR since the number of phonon quanta around the hole is not limited.

The key role of the vertex corrections for e-ph interaction in SCR can be demonstrated by the numerically exact diagrammatic Monte Carlo (DMC) method [20–23], where Feynman graphs for the Matsubara Green function of a hole in phonon bath are generated and summed up without systematic errors. As a test, we studied the two-dimensional Holstein model, where the complete and PPNCA summation can be performed exactly. In this model, the hole freely hops with the amplitude t (t is set to unity below) and interacts with dispersionless (frequency $\Omega = \text{const}$) optical phonons by short range coupling γ:

$$\hat{H}^{e\text{-ph}} = \Omega \sum_{\mathbf{k}} b_{\mathbf{k}}^{\dagger} b_{\mathbf{k}} + N^{-1} \gamma \sum_{\mathbf{k},\mathbf{q}} [h_{\mathbf{k}}^{\dagger} h_{\mathbf{k}-\mathbf{q}} b_{\mathbf{q}} + \text{H.c.}]. \quad (2)$$

Exact and PPNCA results for the energy and the Z factor of the polaron are in good agreement at small values $g \leq 0.2$ of the dimensionless interaction constant $g = \gamma^2/(8t\Omega)$, but are crucially different in the intermediate and strong-coupling regimes. For example, for $\Omega/t = 0.1$, the exact result shows crossover to SCR at $g > g_H^c \approx 0.6$, while in PPNCA the polaron is in the weak coupling regime even for $g = 60$. We conclude that the DMC method is the only method which can treat intermediate and strong-coupling regimes of the e-ph interaction for the problem of one hole in the macroscopic system.

In this Letter, we present a study of a single hole in the t-J model interacting with dispersionless optical phonons (2) by the DMC [20–23] method. We found that, due to slowing down of the hole by the spin flip cloud around it, the hole in the t-J model is subject to the stronger e-ph coupling than the freely propagating hole and, hence, undergoes the crossover to SCR at smaller coupling. This is in contrast to the naive expectation that the small Z factor reduces the e-ph coupling in the t-J model. Besides, we found that SCR occurs at e-ph couplings which are typical for high T_c materials. Finally, our results for SCR qualitatively reproduce data of ARPES experiments: A broad peak, whose energy dispersion is similar to that of the pure t-J model, dominates in the low energy part of LSF.

In the standard spin-wave approximation in momentum representation [24], the dispersionless hole $\varepsilon_0 = \text{const}$ (annihilation operator is $h_{\mathbf{k}}$) propagates in the magnon (annihilation operator is $\alpha_{\mathbf{k}}$) bath:

$$\hat{H}_{t\text{-}J}^{0} = \sum_{\mathbf{k}} \varepsilon_0 h_{\mathbf{k}}^{\dagger} h_{\mathbf{k}} + \sum_{\mathbf{k}} \omega_{\mathbf{k}} \alpha_{\mathbf{k}}^{\dagger} \alpha_{\mathbf{k}}, \quad (3)$$

with magnon dispersion $\omega_{\mathbf{k}} = 2J\sqrt{1-\gamma_{\mathbf{k}}^2}$, where $\gamma_{\mathbf{k}} = (\cos k_x + \cos k_y)/2$. The hole is scattered by magnons,

$$\hat{H}_{t\text{-}J}^{h\text{-}m} = N^{-1} \sum_{\mathbf{k},\mathbf{q}} M_{\mathbf{k},\mathbf{q}} [h_{\mathbf{k}}^{\dagger} h_{\mathbf{k}-\mathbf{q}} \alpha_{\mathbf{q}} + \text{H.c.}], \quad (4)$$

with the scattering vertex $M_{\mathbf{k},\mathbf{q}} = 4t(u_{\mathbf{q}}\gamma_{\mathbf{k}-\mathbf{q}} + v_{\mathbf{q}}\gamma_{\mathbf{k}})$, where $u_{\mathbf{k}} = \sqrt{(1+\nu_{\mathbf{k}})/(2\nu_{\mathbf{k}})}$, $v_{\mathbf{k}} = -\text{sgn}(\gamma_{\mathbf{k}}) \times \sqrt{(1-\nu_{\mathbf{k}})/(2\nu_{\mathbf{k}})}$, and $\nu_{\mathbf{k}} = \sqrt{1-\gamma_{\mathbf{k}}^2}$. We chose the value $J/t = 0.3$ at which NCA for magnons is shown to be a sufficiently good approximation [24] and set the phonon frequency $\Omega = 0.1$ to make it similar to the experimental value [25].

We generate the Feynman expansion of the Matsubara Green function of a hole in momentum representation for the infinite system at zero temperature by the DMC method [21–23]. Then we obtain LSF by the stochastic optimization method [21,26] which resolves equally well both sharp and broad features of the spectra. Diagrams with crossing of a magnon propagator by both magnon and phonon lines are neglected [27] though the diagrams with intercrossing of phonon propagators are taken into account. The DMC algorithm for the pure t-J model Eqs. (3) and (4) is equivalent to the macroscopic limit of the SCBA approach on finite lattices [24]. When PPNCA is introduced to the DMC method at finite couplings to phonons, the algorithm is nothing but the thermodynamic limit of the SCBA approach on finite lattices to the complete model (2)–(4) when both magnons and phonons are taken into account in the NCA [19]. Comparison of our data with results of Refs. [19,24] shows that the Z factor and energy of the lowest peak are weakly influenced by finite size corrections since the relative discrepancy is less than 10^{-2}. The shapes of LSF in the SCBA approach are very similar to those obtained by the DMC method. We observed only a slight discrepancy in widths and energies of high energy peaks. Therefore, the main advantage of the DMC method over other existing methods is the possibility to take into account phonon-phonon vertex corrections in the macroscopic system.

Figure 1 presents our results for LSF in the ground state. Three low energy peaks for $g = 0$ [Fig. 1(a)] are string resonances [28] since their energies, as we found in calculations of LSF for different exchange constants $0.1 \leq J \leq 0.4$, obey the scaling law $a + b_i(J/t)^{2/3}$ ($a = -3.13$, $b_{1,2,3} = 4.89/2.09/1.63$). The lower panel of Fig. 1 shows typical LSF in weak-coupling [Fig. 1(b)], intermediate-coupling [Fig. 1(c)], and strong-coupling [Fig. 1(d)] regimes of interaction with phonons. With an increase of g, three peaks in LSF are observed up to $g = 0.21$ [Figs. 1(b) and 1(c)], while the peak with highest energy broadens and disappears at higher couplings [Fig. 1(d)].

Dependence of the peak energies [Fig. 2(a)] and ground state Z factor [Fig. 2(c)] on g resembles a picture inherent in self-trapping phenomenon [26,29]: The states cross and hybridize at critical coupling $g_{t\text{-}J}^c \approx 0.19$ and the Z factor

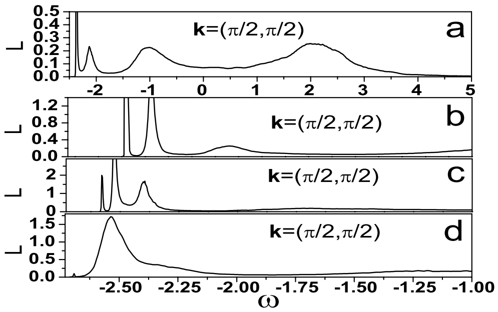

FIG. 1. Hole LSF in ground state at $J/t = 0.3$. (a) For $g = 0$. (b)–(d) Low energy part for $g = 0.1445$ [$\gamma = 0.34$] (b), $g = 0.2$ [$\gamma = 0.4$] (c), and $g = 0.231\,125$ [$\gamma = 0.43$] (d).

of the ground state resonance rapidly decreases. We note that the PPNCA result does not show a transition into SCR even at considerably larger g [see Figs. 2(b) and 2(c)]. According to general understanding of the self-trapping crossover, at small g the ground state is weakly coupled to phonons while excited resonances have a strong lattice deformation. At critical coupling, the crossing and hybridization of these states occurs and for higher g the roles of these states exchange: The lowest state is strongly trapped by lattice deformation while the upper ones are nearly free. Therefore, above the crossover point $g > g^c_{t\text{-}J}$, one expects that the lowest state should be dispersionless while the upper resonances have to show considerable momentum dependence. This assumption is supported by momentum dependence of LSF well above the crossover point (Fig. 3). The energy of the lowest peak is momentum independent while the bandwidth of the upper broad resonance (Fig. 4) is the same ($W_{J/t=0.3} = 0.6$) as it is in the pure t-J model. The most surprising peculiarity of the momentum dependence of broad resonance is that it is exactly the same as expected for the t-J model with no coupling to phonons: It obeys the scaling relation

$$\varepsilon_{\mathbf{k}} = \varepsilon_{\min} + W_{J/t}\{[\cos k_x + \cos k_y]^2/5 + [\cos(k_x + k_y) + \cos(k_x - k_y)]^2/4\}, \tag{5}$$

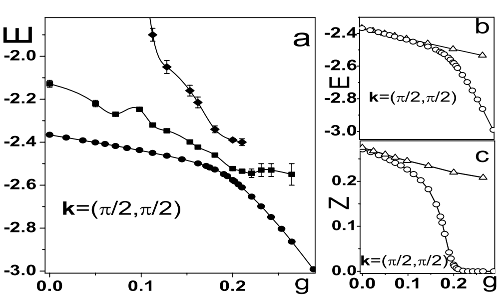

FIG. 2. Dependence on coupling strength at $J/t = 0.3$. (a) Energies of lowest LSF resonances. (b) [(c)] energy [Z factor] of lowest peak in DMC (circles) and PPNCA (triangles). Lines are to guide the eye. The error bar, if not shown, is less than the point size.

which describes dispersion for the pure t-J model in the broad range of exchange constants $0.1 \leq J/t \leq 0.9$ [30]. We emphasize that unrenormalized dispersion of the upper resonances is the general property of SCR. For example, for the coupling $g = 0.2$, which is slightly higher than the critical coupling $g^c_{t\text{-}J}$ [see Figs. 1(c) and 2], dispersion of the upper resonance also obeys Eq. (5) while the lowest peak is momentum independent (see Fig. 4). Such behavior of upper resonance indicates that an argument of weak coupling theory [31] can be qualitatively extended to the SCR. With an increase of the energy, the pole renormalization (real part of the self energy) rapidly decreases above the phonon frequency while the broadening (imaginary part of the self-energy) saturates at a maximal value.

The behavior of LSF in SCR is exactly the same as observed in ARPES experiments. The LSF consists of *broad QP* peak and high-energy incoherent continuum (see Fig. 3). Besides, momentum dependence of the broad QP peak is similar to dispersion of sharp resonance in the pure t-J model (see Fig. 4). The lowest lying dispersionless peak in SCR has a small Z factor and cannot be discerned in ARPES experiments: Its spectral weight is small ($Z \sim 0.015$) at $g = 0.2$ [Fig. 1(c)] and completely suppressed ($Z < 10^{-3}$) at $g = 0.231\,125$ [Fig. 1(d)]. On the other hand, the momentum dependence of spectral weight Z' of broad dispersive resonance in SCR is akin to that in the pure t-J model. For $g = 0.231\,125$, the weights of the broad peak at $\mathbf{k} = (\pi/2, \pi/2)$ ($\sim$0.27) and at $\mathbf{k} = (0, 0)$ ($\sim$0.05) coincide with Z factors of sharp resonances at corresponding momenta in the pure t-J model. Our calculations show that this similarity is the robust feature of SCR: $Z'_{(\pi/2,\pi/2)} \sim 0.27 \pm 0.01$ and $Z'_{(0,0)} \sim 0.05 \pm 0.005$ in the broad range of coupling constants $0.21 < g < 0.27$.

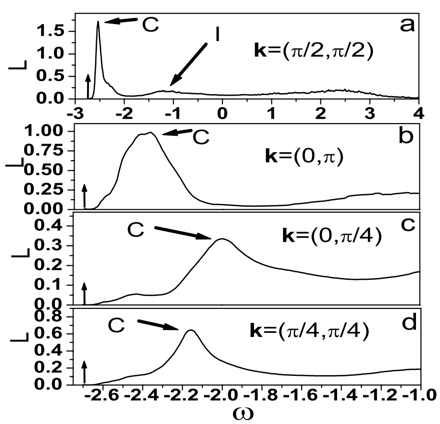

FIG. 3. LSF of the hole at $J/t = 0.3$ and $g = 0.231\,125$. (a) Full energy range for $\mathbf{k} = (\pi/2, \pi/2)$. (b)–(d) Low energy part for different momenta. Slanted arrows show broad peaks which can be interpreted in ARPES spectra as coherent (C) and incoherent (I) part. Vertical arrows indicate position of ground state resonance which is not seen in the vertical scale of the figure.

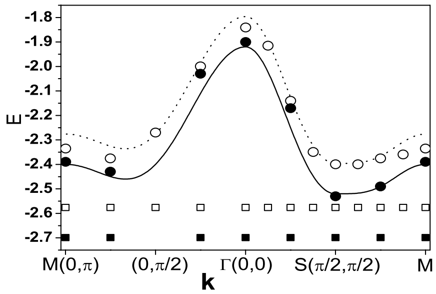

FIG. 4. Dispersion of resonance energies at $J/t = 0.3$. Broad resonance (filled circles) and lowest polaron resonance (filled squares) at $g = 0.231\,125$; third broad resonance (open circles) and lowest polaron resonance (open squares) at $g = 0.2$. The solid curves are dispersions (5) of a hole in the pure t-J model at $J/t = 0.3$ ($W_{J/t=0.3} = 0.6$): $\varepsilon_{\min} = -2.396$ ($\varepsilon_{\min} = -2.52$) for solid (dotted) line.

Comparing the critical interaction $g^c_{t\text{-}J} \approx 0.19$ for the hole in the t-J model and critical coupling $g^c_H \approx 0.6$ for the Holstein model with the same value of hopping t, we conclude that interaction with spins enhances e-ph coupling and accelerates transition into SCR. Emission of magnons on each hopping shrinks the bandwidth of lowest lying resonance by the factor of J/t while the reduction of the e-ph vertex by the factor Z seems to be absent. This makes the influence of the e-ph interaction on the low energy part of LSF more effective. We emphasize that the critical interaction for transition to SCR is low enough for the t-J model to bring the realistic system into SCR. For example, a theoretical estimate of the interaction strength from the fitting of phonon energies and line shapes to the neutron scattering experiment gives a rather large magnitude for e-ph coupling in $La(Sr)CuO_4$ [15]. Since the interaction vertex is momentum dependent in the model [15], we can establish only lower and upper bounds for effective coupling g in our model with a short-range interaction. The averaging over the Brillouin zone gives the lower bound $g^{\min}_{\exp} \geq 0.15$ while the maximal value at the Brillouin zone boundary determines the upper bound $g^{\max}_{\exp} \leq 0.5$. However, since self-trapping is governed mainly by short-range coupling [29], an effective constant in our model is closer to the upper bound $g^{\max}_{\exp}$. Thus, realistic high T_c cuprates are expected to be in SCR.

Finally, we conclude that puzzling behavior of ARPES spectra in undoped high T_c materials, which manifests itself in an unexpectedly *broad* QP peak with dispersion corresponding to the pure Mott insulator model, is driven by strong electron-phonon interaction.

Fruitful discussions with N.V. Prokof'ev, B.V. Svistunov, G. Khaliullin, and G. A. Sawatzky are acknowledged. This work was supported by RFBR 04-02-17363a.

[1] C. L. Kane, P. A. Lee, and N. Read, Phys. Rev. B **39**, 6880 (1989).
[2] E. Manousakis, Rev. Mod. Phys. **63**, 1 (1991);E. Dagotto, *ibid.* **66**, 763 (1994).
[3] M. Brunner, F. F. Assaad, and A. Muramatsu, Phys. Rev. B **62**, 15 480 (2000).
[4] A. S. Mishchenko, N V. Prokofév, and B.V. Svistunov, Phys. Rev. B **64**, 033101 (2001).
[5] J. Bała, A. M. Oleś, and J. Zaanen, Phys. Rev. B **52**, 4597 (1995).
[6] T. Xiang and M. Wheatley, Phys. Rev. B **54**, R12 653 (1996).
[7] B. Kyung and R. A. Ferrell, Phys. Rev. B **54**, 10 125 (1996).
[8] T. K. Lee and C. T. Shih, Phys. Rev. B **55**, 5983 (1997).
[9] T. K. Lee, C.-M. Ho, and N. Nagaosa, Phys. Rev. Lett. **90**, 067001 (2003).
[10] T. Tohyama and S. Maekawa, Supercond. Sci. Technol. **13**, R17 (2000).
[11] A. Danmascelli, Z.-X. Shen, and Z. Hussain, Rev. Mod. Phys. **75**, 473 (2003).
[12] B. O. Wells *et al.*, Phys. Rev. Lett.**74**, 964 (1995).
[13] S. Yunoki, A. Macridin, and G. A. Sawatzky (private communication).
[14] A. S. Mishchenko and N. Nagaosa (unpublished).
[15] P. Horsch and G. Khaliullin, in *Open Problems in Strongly Correlated Electron Systems*, edited by J. Bonca *et al.* (Kluwer Academic, Boston, 2001), p. 81.
[16] J. Hofer *et al.*, Phys. Rev. Lett. **84**, 4192 (2000).
[17] B. Bauml, G. Wellein, and H. Fehske, Phys. Rev. B **58**, 3663 (1998).
[18] A. Ramsak, P. Horsch, and P. Fulde, Phys. Rev. B **46**, 14 305 (1992).
[19] B. Kyung *et al.*, Phys. Rev. B **54**, 13 167 (1996).
[20] N.V. Prokof'ev and B.V. Svistunov, Phys. Rev. Lett. **81**, 2514 (1998).
[21] A. S. Mishchenko *et al.*, Phys. Rev. B **62**, 6317 (2000).
[22] A. S. Mishchenko and N. Nagaosa, Phys. Rev. Lett. **86**, 4624 (2001).
[23] A. S. Mishchenko *et al.*, Nonlinear Opt **29**, 257 (2002).
[24] Z. Liu and E. Manousakis, Phys. Rev. B **45**, 2425 (1992).
[25] The value of t varies for high T_c materials in an energy scale $t \approx 0.3$–0.43 eV [2,6] while the energy of phonons which interact with the hole is lower than 55–80 meV [11]. We found that variation of parameter Ω/t within the adopted [15,18,19] range 0.1–0.2 has no significant influence on results.
[26] A. S. Mishchenko *et al.*, Phys. Rev. B **66**, 020301 (2002).
[27] This approximation is necessary to avoid a sign problem arising from the momentum dependence of $M_{\mathbf{k},\mathbf{q}}$.
[28] B. I. Shraiman and E. Sigga, Phys. Rev. Lett. **60**, 740 (1988).
[29] E. I. Rashba, *Self-Trapping of Excitons*, in Modern Problems in Condensed Matter Sciences, edited by V. M. Agranovich and A. A. Maradudin (North-Holland, Amsterdam, 1982), Vol. 2, p. 543.
[30] F. Marsiglio *et al.*, Phys. Rev. B **43**, 10 882 (1991).
[31] G. Grimvall, *The Electron-Phonon Interaction in Metals* (North-Holland, New York, 1981).